

MSSM Predictions for  $B^0 \rightarrow \mu^+ \mu^-$  at Tevatron and LHC\*

JANUSZ ROSIEK

Institute of Theoretical Physics, University of Warsaw

During the last few years the Tevatron has improved the bounds on rare  $B$ -meson decays into two leptons. Sensitivity to this decay is also one of the benchmark goals for LHCb performance. We compute the complete 1-loop MSSM contribution to  $B_{s,d}^0 \rightarrow \mu^+ \mu^-$  and study the predictions for arbitrary flavour mixing parameters. We discuss the possibility of both enhancing and suppressing the branching ratios relative to their SM expectations. We find that there are ‘‘cancellation regions’’ in parameter space where the branching ratio is suppressed well below the SM expectation, making it effectively invisible to the LHC.

PACS numbers: 12.60.Jv; 12.15.Ff; 13.20.He

## 1. Introduction

One of the most promising signals for new physics at the LHC is the rare decay  $B_s^0 \rightarrow \mu^+ \mu^-$ . The decay is strongly suppressed but especially ‘clean’ because its final state is easily tagged and its only hadronic uncertainties come from the hadronic decay constant  $f_{B_s}$  [1]. The LHC will be the first experiment to be able to probe this decay channel down to its Standard Model (SM) branching ratio. In particular the LHCb will be able to directly probe the SM predictions at  $3\sigma$  ( $5\sigma$ ) significance with  $2 \text{ fb}^{-1}$  ( $6 \text{ fb}^{-1}$ ) of data, or after about 1 year (3 years) of design luminosity [2]. It is not clear whether LHC can reach the SM expectation for  $B_d^0 \rightarrow \mu^+ \mu^-$ .

The current experimental status and the SM predictions for the branching ratios  $B_{s,d}^0 \rightarrow \mu^+ \mu^-$  are:

Channel	Expt.	Bound (90% CL)	SM Prediction
$B_s^0 \rightarrow \mu^+ \mu^-$	CDF II [3]	$< 4.7 \times 10^{-8}$	$(4.8 \pm 1.3) \times 10^{-9}$
$B_d^0 \rightarrow \mu^+ \mu^-$	CDF II [3]	$< 1.5 \times 10^{-8}$	$(1.4 \pm 0.4) \times 10^{-10}$

At the dawn of the LHC era, it is important to understand the possible contributions of new physics to the  $B_{s,d}^0 \rightarrow \mu^+ \mu^-$  decays. They could be

\* Presented at the FlaviaNet Topical Workshop, 23-27 July 2009, Kazimierz, Poland.

particularly large in the Minimal Supersymmetric Standard Model (MSSM). Under the assumption of large  $\tan\beta$  and Minimal Flavour Violation (MFV, flavour violation given by CKM matrix only), the branching ratio for  $B_s^0 \rightarrow \mu^+\mu^-$  is dominated by the Higgs penguin mode and can be significantly enhanced over the SM expectation, as can be seen from the approximate formulae (for detailed study focusing on the resummation of  $\tan\beta$  see [4]):

$$\mathcal{B}(B_s^0 \rightarrow \mu^+\mu^-) \approx 5 \cdot 10^{-7} \left(\frac{\tan\beta}{50}\right)^6 \left(\frac{300 \text{ GeV}}{M_A}\right)^4. \quad (1)$$

With the upcoming new experimental probes of  $\mathcal{B}(B_{s,d}^0 \rightarrow \mu^+\mu^-)$ , it is important to perform a full calculation of this decay rate without *a priori* assumptions on the pattern of flavour mixing. In particular, in the region of low  $\tan\beta$ , the interference of box,  $Z$ - and Higgs-penguin diagrams could conceivably lead to both enhancement (even visible at Tevatron) or a cancellation that would suppress the branching ratio below the SM prediction (making it invisible at the LHC). The status of this decay could become an important factor for planned LHCb upgrades and determining whether they should focus on increasing sensitivity to  $B_s^0 \rightarrow \mu^+\mu^-$  or instead reach for the smaller branching ratio of  $B_d^0 \rightarrow \mu^+\mu^-$ . The relevant calculations have been presented in details in [5], we stress here the most important results.

## 2. Effective Operators and Branching Ratios

The effective Hamiltonian for the quarks-to-leptons transition  $q^I q^J \rightarrow \ell^{+K} \ell^{-L}$ , with  $q^1 \equiv d, q^2 \equiv s, q^3 \equiv b$  and  $\ell^1 \equiv e, \ell^2 \equiv \mu, \ell^3 \equiv \tau$ , reads:

$$\mathcal{H} = \frac{1}{(4\pi)^2} \sum_{X,Y=L,R} \left( C_{VXY} \mathcal{O}_{VXY} + C_{SXY} \mathcal{O}_{SXY} + C_{TX} \mathcal{O}_{TX} \right), \quad (2)$$

where flavour and colour indices have been suppressed for brevity. The (V)ector and (S)calar operators are respectively given by

$$\begin{aligned} \mathcal{O}_{VXY}^{IJKL} &= (\bar{q}^J \gamma^\mu P_X q^I) (\bar{\ell}^L \gamma_\mu P_Y \ell^K), \\ \mathcal{O}_{SXY}^{IJKL} &= (\bar{q}^J P_X q^I) (\bar{\ell}^L P_Y \ell^K). \end{aligned} \quad (3)$$

The explicit form of the Wilson coefficients in the MSSM is given in [5]. The (T)ensor operator contributions and photon penguin contribution to  $B_s^0 \rightarrow \ell^+ \ell'^-$  vanishes in matrix element calculations. We do not consider the very large  $\tan\beta \gtrsim 30$  scenario, thus no resummation of higher orders in  $\tan\beta$  is necessary. The matrix element for  $B_{s,d}^0 \rightarrow \ell^+ \ell'^-$  decay is:

$$\mathcal{M} = F_S \bar{\ell} \ell + F_P \bar{\ell} \gamma_5 \ell + F_V p^\mu \bar{\ell} \gamma_\mu \ell + F_A p^\mu \bar{\ell} \gamma_\mu \gamma_5 \ell, \quad (4)$$

where the  $\ell$ s correspond to external lepton spinors. The (S)calar, (P)seudo-scalar, (V)ector and (A)xial-vector form factors in Eq. (4) are given by

$$F_S = \frac{i}{4} \frac{M_{B_{s(d)}}^2 f_{B_{s(d)}}}{m_b + m_{s(d)}} (C_{SLL} + C_{SLR} - C_{SRR} - C_{SRL}), \quad (5)$$

$$F_P = \frac{i}{4} \frac{M_{B_{s(d)}}^2 f_{B_{s(d)}}}{m_b + m_{s(d)}} (-C_{SLL} + C_{SLR} - C_{SRR} + C_{SRL}), \quad (6)$$

$$F_V = -\frac{i}{4} f_{B_{s(d)}} (C_{VLL} + C_{VLR} - C_{VRR} - C_{VRL}), \quad (7)$$

$$F_A = -\frac{i}{4} f_{B_{s(d)}} (-C_{VLL} + C_{VLR} - C_{VRR} + C_{VRL}). \quad (8)$$

The general expression for  $\mathcal{B}(B_{s,d}^0 \rightarrow \ell^+ \ell^-)$  is rather complicated [5]. For the most important  $B_{s,d}^0 \rightarrow \mu^+ \mu^-$  decays it simplifies greatly and reads approximately as ( $q = s, d$ )

$$\mathcal{B}(B_q^0 \rightarrow \mu^- \mu^+) \approx \frac{\tau_{B_q} M_{B_q}}{8\pi} (|F_S|^2 + |F_P + 2m_\mu F_A|^2), \quad (9)$$

where  $\tau_{B_q}$  is the lifetime of  $B_q$  meson and we have taken the limit  $\frac{m_\mu}{M_{B_q}} \rightarrow 0$ .

### 3. Numerical Analysis of $B_{s,d} \rightarrow \mu^+ \mu^-$

We may distinguish two possible scenarios for the relative size of the MSSM contributions to the right-hand side of Eq. (9):

1. *Higgs penguin domination or large  $\tan \beta \gtrsim 10$ .* In this regime one can expect large  $F_S, F_P$  and an enhancement of the branching ratios as in Eq. (1) (barring some possible GIM-type cancellations leading to  $F_{S,P}^{\text{SUSY}} \approx 0$  [6]).
2. *Comparable Box, Z- and Higgs-penguin contributions or low  $\tan \beta \lesssim 10$ .* In this case the supersymmetric Higgs-mediated form factors  $F_{S,P}$  may become comparable to or even smaller than  $F_A$ . Either an enhancement or a suppression of the branching ratios is possible depending on the particular choice of MSSM parameters.

An enhancement of the branching ratios occurs generically in most of the MSSM parameter space. It is a bit trickier to suppress the branching ratios below their SM predictions. This is the case we would like to investigate further. We would like to find the minima of  $\mathcal{B}(B_{s,d}^0 \rightarrow \mu^+ \mu^-)$ , i.e. the minima of Eq. (9). We distinguish between two cases:

$$a) \quad F_P + 2m_\ell F_A \approx 0 \quad \text{and} \quad F_P \gg F_S, \quad (10)$$

$$a) \quad |F_S| \approx |F_P| \approx |F_A| \approx 0. \quad (11)$$

In the case a), the pseudoscalar and axial contributions cancel while the scalar contribution is negligible. The case b), happens when Higgs contributions are negligible compared to the axial contribution (i.e. low  $\tan \beta$  and large  $M_A$ ) and  $F_A$  becomes small due to cancellations among the  $C_{VXY}$  coefficients in Eq. (8). Our numerical analysis shows that both can-

**Table 1**

Parameter	Symbol	Min	Max	Step
Ratio of Higgs vevs	$\tan \beta$	2	30	varied
CKM phase	$\gamma$	0	$\pi$	$\pi/25$
CP-odd Higgs mass	$M_A$	100	500	200
SUSY Higgs mixing	$\mu$	-450	450	300
$SU(2)$ gaugino mass	$M_2$	100	500	200
Gluino mass	$M_3$	$3M_2$	$3M_2$	0
SUSY scale	$M_{\text{SUSY}}$	500	1000	500
Slepton Masses	$M_{\tilde{\ell}}$	$M_{\text{SUSY}}/3$	$M_{\text{SUSY}}/3$	0
Left top squark mass	$M_{\tilde{Q}_L}$	200	500	300
Right bottom squark mass	$M_{\tilde{b}_R}$	200	500	300
Right top squark mass	$M_{\tilde{t}_R}$	150	300	150
Mass insertion	$\delta_{dLL}^{13}, \delta_{dLL}^{23}$	-1	1	1/10
Mass insertion	$\delta_{dLR}^{13}, \delta_{dLR}^{23}$	-0.1	0.1	1/100

cellations are possible but require a certain amount of fine tuning once constraints from other FCNC measurements are imposed.

To quantitatively study the effects mentioned above we perform a scan over the MSSM parameters, not restricted to MFV scenario. Flavour violation is parametrised by the “mass insertions”, defined as in [7, 8]

$$\delta_{QXY}^{IJ} = \frac{(M_Q^2)_{XY}^{IJ}}{\sqrt{(M_Q^2)_{XX}^{IJ}(M_Q^2)_{YY}^{IJ}}}, \quad (12)$$

where  $I, J$  are squark flavours,  $X, Y$  denote field chirality, and  $Q$  indicates the up or down squark sector. Note that we use the  $\delta$ 's for presentation only, not as expansion parameters - we numerically diagonalize all mass matrices.

The ranges of variation over MSSM parameters are shown in Table 1, where “SUSY scale” denotes the common mass parameter for the first two squark generations,  $\tan \beta$  takes on values (2, 4, 6, 8, 10, 13, 16, 19, 22, 25, 30),  $\delta_{dLL}^{IJ}, \delta_{dLR}^{IJ}, \mu, M_2$  are taken to be real and the trilinear soft couplings are set to  $A_t = A_b = M_{\tilde{Q}_L}$  and  $A_{\tilde{\tau}} = M_{\tilde{L}}$ .

To realistically estimate the allowed range for  $\mathcal{B}(B_{s,d}^0 \rightarrow \mu^+ \mu^-)$ , one must account for the experimental constraints from other rare decays. For that, we use the library of numerical codes developed in the framework of the general MSSM in [4, 5, 8, 9, 10] and take into account the set of observables listed in Table 2<sup>1</sup>. In our scan, for the quantities in Table 2 we require (depending if the experimental result or only the upper bound is known)

$$\begin{aligned} & |Q^{exp} - Q^{th}| \leq 3\Delta Q^{exp} + q|Q^{th}|, \\ \text{or} & \\ & (1+q)|Q^{th}| \leq Q^{exp}. \end{aligned} \quad (13)$$

<sup>1</sup> For Higgs mass we use LEP data [11]  $m_h \geq 92.8 - 114$  GeV depending on  $\sin^2(\alpha - \beta)$ .

**Table 2**

Quantity	Current Measurement	Experimental Error
$m_{\chi_1^0}$	$> 46$ GeV	
$m_{\chi_1^\pm}$	$> 94$ GeV	
$m_{\tilde{b}}$	$> 89$ GeV	
$m_{\tilde{t}}$	$> 95.7$ GeV	
$m_h$	$> 92.8$ GeV	
$ \epsilon_K $	$2.232 \cdot 10^{-3}$	$0.007 \cdot 10^{-3}$
$ \Delta M_K $	$3.483 \cdot 10^{-15}$	$0.006 \cdot 10^{-15}$
$ \Delta M_D $	$< 0.46 \cdot 10^{-13}$	
$\Delta M_{B_d}$	$3.337 \cdot 10^{-13}$ GeV	$0.033 \cdot 10^{-13}$ GeV
$\Delta M_{B_s}$	$116.96 \cdot 10^{-13}$ GeV	$0.79 \cdot 10^{-13}$ GeV
$\text{Br}(B \rightarrow X_s \gamma)$	$3.34 \cdot 10^{-4}$	$0.38 \cdot 10^{-4}$
$\text{Br}(K_L \rightarrow \pi^0 \nu \bar{\nu})$	$< 1.5 \cdot 10^{-10}$	
$\text{Br}(K^+ \rightarrow \pi^+ \nu \bar{\nu})$	$1.5 \cdot 10^{-10}$	$1.3 \cdot 10^{-10}$
Electron EDM	$< 0.07 \cdot 10^{-26}$	
Neutron EDM	$< 0.63 \cdot 10^{-25}$	

$3\Delta Q^{exp}$  and  $|qQ^{th}|$  in Eq. (13) represent the  $3\sigma$  experimental error and the theoretical error respectively. The latter differs from quantity to quantity and is usually smaller than the value  $q = 50\%$  which we assume generically in all calculations. The increased ‘‘theoretical error’’ is used to account for the limited density of a numerical scan, simultaneously avoiding strong fine tuning between MSSM parameters (for detailed discussion see [10]).

Fig. 1 shows the predictions for  $\mathcal{B}(B_s^0 \rightarrow \mu^+ \mu^-)$  over a general scan of 20 million points in parameter space, including the bounds of Table 2. We vary  $\delta_{dLL}^{23}$  (upper panel) and  $\delta_{dLR}^{23}$  (lower panel) one at a time while setting the other to zero (results are also weakly sensitive to other  $\delta$ 's). When  $\delta_{dLL}^{23}$  is varied in the range  $[-1, 1]$ , we find  $\mathcal{B}(B_s^0 \rightarrow \mu^+ \mu^-)_{min} \approx 10^{-9}$ . This minimum is almost independent of  $\tan \beta$  but depends on the magnitude of  $|\delta_{dLL}^{23}|$ . The upper bound set by CDF, depicted as a solid red line, can be attained even with very low values of  $\tan \beta$ .

More interesting is the case when  $\delta_{dLR}^{23}$  is varied in the range  $[-0.1, 0.1]$ . We find a narrow cancellation region around  $\delta_{dLR}^{23} \approx -0.01$  and  $\tan \beta \lesssim 10$  where  $\mathcal{B}(B_s^0 \rightarrow \mu^+ \mu^-)_{min} \approx 10^{-12}$  (lower right panel). This is three orders of magnitude lower than the SM prediction, making it effectively unobservable at the LHC. In order to better understand cancellation region we study a representative point with a very low branching ratio (all masses in GeV):

$$\begin{aligned} \tan \beta = 4, \quad M_A = 300, \quad \mu = -450, \quad M_2 = 100, \quad M_3 = 300, \\ \text{SUSY scale} = 400, \quad M_{\tilde{t}_R} = 150, \quad A_{t,b} = M_{\tilde{t}_L} = M_{\tilde{b}_{(L,R)}} = 600. \end{aligned} \quad (14)$$

The ‘Box’, ‘Higgs’ and ‘Z’ lines in Fig. 2 indicate the value of  $\mathcal{B}(B_s^0 \rightarrow \mu^+ \mu^-)$  given by only the listed contribution with all others set to zero. In the cancellation region the box contribution is negligible while the Higgs- and Z-

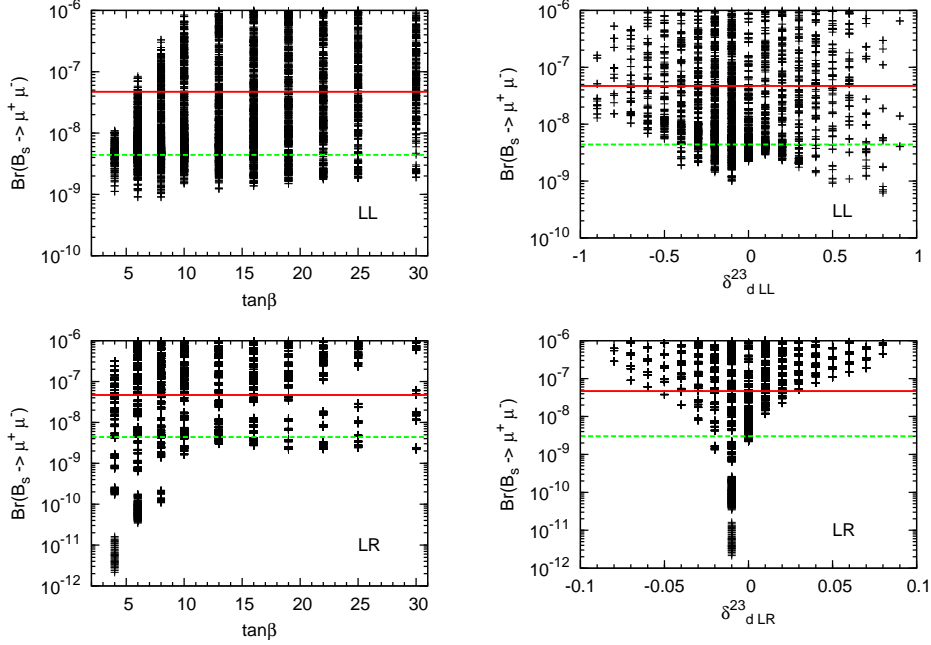


Fig. 1. Upper panel: Predictions for  $\mathcal{B}(B_s \rightarrow \mu^+ \mu^-)$  versus  $\tan \beta$  (left) and  $\delta_{dLL}^{23}$  (right) from the scan of MSSM parameters. The upper solid line shows the current upper bound from the Tevatron and the lower dashed line the SM expectation. Lower panel: Similar to the upper panel but with  $\delta_{dLR}^{23}$  varied.

penguin magnitudes are comparable. Thus the latter should cancel, which we illustrate individually plotting the absolute values of the form factors  $F_{S,P}$  and  $2m_\mu F_A$  of Eqs. (5–8) in the right panel of Fig. 2. At the minimum point of the total branching ratio  $|F_P|$  is approximately equal to  $|2m_\mu F_A|$  and  $|F_S|$  is negligibly small. This can be explained from the form of Eqs. (5) and (6). If one assumes  $\delta_{dLR}^{23} = (\delta_{dLR}^{32})^*$ , then  $C_{SLR}$  and  $C_{SRL}$ , the two Wilson coefficients most sensitive to the variation of  $\delta_{dLR}^{23}$ , have similar sizes and opposite sign, interfering destructively in the amplitude.

We performed similar scan also for the  $B_d$  meson decay,  $B_d \rightarrow \mu^+ \mu^-$ , varying  $\delta_{dLL}^{13}$  or  $\delta_{dLR}^{13}$  instead of  $\delta_{dLL}^{23}$  or  $\delta_{dLR}^{23}$  along with the other SUSY parameters. For both cases there exist points where  $\mathcal{B}(B_d \rightarrow \mu^+ \mu^-)$  is reduced by an order of magnitude relative to the SM. These points are more sensitive to low  $\tan \beta$  in the ‘LL’ case and fall into the case of Eq. (11). On the opposite, the ratio  $R = \mathcal{B}(B_d \rightarrow \mu^+ \mu^-)/\mathcal{B}(B_s \rightarrow \mu^+ \mu^-)$ , which in the SM is fixed to  $R \approx |V_{td}/V_{ts}|^2 \leq 0.03$ , in the MSSM can be enhanced by a factor of 10 even for small values of  $\delta_{dLL}^{13}$  or  $\delta_{dLR}^{13}$ . This suggests that collider searches for  $\mathcal{B}(B_d \rightarrow \mu^+ \mu^-)$  are as important as those for  $\mathcal{B}(B_s \rightarrow \mu^+ \mu^-)$ .

Our results lead also to bounds on  $\delta$  parameters. As can be seen from

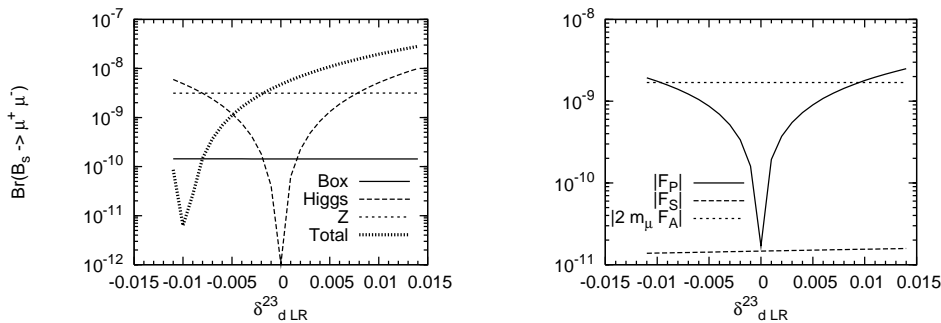


Fig. 2. Contributions to  $\mathcal{B}(B_{s,d}^0 \rightarrow \mu^+ \mu^-)$  for the parameters in Eq. (14) versus  $\delta_{dLR}^{23}$ . Left: Contributions from the various diagram classes. Right: Magnitude of the form factors appearing in Eqs. (5–8).

Figs 1 and scan results for  $\mathcal{B}(B_d \rightarrow \mu^+ \mu^-)$ ,  $\delta_{dLL}^{23}, \delta_{dLL}^{13}$  are weakly constrained, they can take on values up to  $\approx 0.9$  and still pass the constraints in Table 2, though points beyond 0.3 are less dense. Bounds in the 'LR' sector are tighter,  $\delta_{dLR}^{23}, \delta_{dLR}^{13} \lesssim 0.08$ .

#### 4. Conclusions

We have discussed results of a complete, 1-loop calculation of the branching ratios for the rare decay modes  $B_{s,d}^0 \rightarrow \mu^+ \mu^-$  without resorting to the limits of large  $\tan\beta$  and MFV scenario and performed a numerical exploration of the MSSM parameter space. We find that there exist cancellation regions where the contribution of diagrams with supersymmetric particles interferes destructively with purely SM diagrams, thus allowing the branching ratio to be significantly smaller than the SM prediction. We identify possible mechanisms of such cancellations and explain why they can occur for certain regions of parameter space. Such effects may effectively hide the dimuon  $B_s^0$  decay mode from the LHCb even though it is supposed to be one of the experiment's benchmark modes. We have also shown that, barring the cancellations mentioned above, supersymmetric contributions in the general MSSM typically tend to enhance the branching ratio for  $B_{s,d}^0 \rightarrow \mu^+ \mu^-$  even for moderate values of  $\tan\beta \lesssim 10$  so that an experimental measurement close to the SM prediction would put strong bounds on the size of allowed flavour violation in the squark sector. Finally, we show that the  $B_d^0 \rightarrow \mu^+ \mu^-$  decay can also be either suppressed or enhanced compared to its SM expectation, leading in some cases to a situation where the rate of the  $B_d^0$  decay is larger than that of the  $B_s^0$ .

**Acknowledgements.** The paper was supported in part by the RTN European Programme, MRTN-CT-2006-035505 (HEPTOOLS, Tools and Precision Calculations for Physics Discoveries at Colliders) and by the Polish Ministry of Science and Higher Education Grant N N202 230337.

## REFERENCES

- [1] G. Buchalla and A. J. Buras, Nucl. Phys. B **400**, 225 (1993).
- [2] M. Lenzi, arXiv:0710.5056 [hep-ex].
- [3] T. Aaltonen *et al.* [CDF Collaboration], Phys. Rev. Lett. **100**, 101802 (2008).
- [4] A. J. Buras, P. H. Chankowski, J. Rosiek and L. Ślawianowska, Nucl. Phys. B **659**, 3 (2003).
- [5] A. Dedes, J. Rosiek and P. Tanedo, Phys. Rev. D **79** (2009) 055006.
- [6] A. Dedes and A. Pilaftsis, Phys. Rev. D **67**, 015012 (2003); J. R. Ellis, J. S. Lee and A. Pilaftsis, Phys. Rev. D **76**, 115011 (2007).
- [7] F. Gabbiani, E. Gabrielli, A. Masiero and L. Silvestrini, Nucl. Phys. B **477**, 321 (1996).
- [8] M. Misiak, S. Pokorski and J. Rosiek, Adv. Ser. Direct. High Energy Phys. **15**, 795 (1998).
- [9] J. Rosiek, Acta Phys. Polon. B **30** (1999) 3379; S. Pokorski, J. Rosiek and C. A. Savoy, Nucl. Phys. B **570** (2000) 81; A. J. Buras, P. H. Chankowski, J. Rosiek and L. Ślawianowska, Nucl. Phys. B **619** (2001) 434; J. Rosiek, arXiv:hep-ph/0108226. A. J. Buras, P. H. Chankowski, J. Rosiek and L. Ślawianowska; Phys. Lett. B **546** (2002) 96; P. H. Chankowski and J. Rosiek, Acta Phys. Polon. B **33** (2002) 2329 [arXiv:hep-ph/0207242].
- [10] A. J. Buras, T. Ewerth, S. Jäger and J. Rosiek, Nucl. Phys. B **714**, 103 (2005).
- [11] S. Schael *et al.* [ALEPH Collaboration and DELPHI Collaboration and L3 Collaboration and ], Eur. Phys. J. C **47** (2006) 547.